Design of optimum roof support systems in South African collieries using a probabilistic design approach

by I. Canbulat* and J.N. van der Merwe†

Synopsis

When designing coal mine roof support, it is necessary to account for the uncertainties and variability that inherently exist within the rock mass and support elements. The performance of a support system is affected by these uncertainties, which are not taken into account in the current deterministic design methodologies used in South Africa.

The key to the design of a roof support system is a better understanding of roof behaviour and uncertainties that can be encountered during extraction. This paper sets out to develop a method that takes all uncertainties that exist within the rock mass and the mining process into account and provides a quantitative risk-based design methodology.

Introduction

Since the introduction of mechanical bolts in the coal mines, the amount of research into the understanding of the behaviour of roof bolts has been significant. Today, almost all coal mine roofs are supported with roof bolts in South Africa. However, falls of ground still remain a major cause of fatalities and injuries in South African collieries.

In the early years, the design of roof bolt patterns was based on local experience and the judgement of mining personnel. The suspension mechanism was the most easily understood and most widely used roof bolting mechanism. However, significant advances have been made over the last 20 years, in particular, the development of resin anchors, tendon elements, and installation hardware. These advances have resulted in an increase in the use of full column resin bolts.

The design of roof bolt patterns has also been improved, and four main rock reinforcement techniques have been developed: simple skin control, beam building, suspension, and keying. In traditional deterministic roof bolt design methodologies, the input parameters are represented using single values. These values are described typically either as 'best guess' or 'worse case' values. However, investigations into the roof and roof bolt behaviour presented by many studies (Van der Merwe[22], Canbulat and Jack[3], Canbulat *et al.*[5], Canbulat *et al.*[6]) suggest that the input parameters, including the mining geometries, rock and support properties can vary significantly within a few metres in a panel and also from one support product to another.

These properties can be described using deterministic (calculation of a single safety factor) and/or probabilistic models. Deterministic models typically use a single discrete descriptor for the parameter of interest. Probabilistic models, however, describe parameters by using discrete statistical descriptors or probability distribution (density) functions. This is the fundamental principle of probabilistic design approach, which is the recognition that the factors that govern the roof stability and support performance exhibit some degree of natural uncertainty.

This uncertainty should ideally be accounted for in the design method. While deterministic approaches provide some insight into the underlying mechanisms, they cannot quantitatively address the risks and uncertainties that are inherently present. In a probabilistic design method, however, the stochastic nature of the input parameters are included and, therefore, it is possible to quantitatively represent uncertainties and thus the resulting probability of failures.

In the paper, a review of the probabilistic approach will be given, followed by an attempt to understand the roof behaviour in South African collieries through *in situ* monitoring.

* *Anglo Coal Australia.*

† *University of Pretoria*

© *The Southern African Institute of Mining and Metallurgy, 2008. SA ISSN 0038–223X/3.00 + 0.00.* *Paper received February 2008; revised paper received February 2009.*

The variability of input parameters will be demonstrated and then a probabilistic model, which describes both the strength and the load acting on rock, will be defined using the stochastic modelling technique. Finally, the application of the model will be demonstrated by a case study.

Review of probabilistic design approach

Rules of probability

The first rule of a probabilistic approach is that all probabilities are numbers between 0 and 1. A probability of 0 indicates an impossible event, and a probability of 1 indicates an event certain to happen. Most events of interest have probabilities that fall between these extremes.

The second rule states that, if two events are dependent (i.e., knowing the outcome of one provides information concerning that the other will occur), then the probability that both events will occur is given by the product of their combined probabilities. Assume, E_1 and E_2 are two events and the event that both E_1 and E_2 occur is described as $P[E_1 E_2]$ and is calculated:

$$P[E_1 E_2] = P[E_1] \times P[E_2/E_1] \quad [1]$$

where $P[E_2/E_1]$ is the probability of E_2 occurring given that E_1 has taken place. If E_1 and E_2 are independent, that is the occurrence of one does not affect the probability of occurrence of the other, the probability of two independent events occurring is the product of their individual probabilities:

$$P[E_2/E_1] = P[E_2] \quad [2]$$

$$P[E_1 E_2] = P[E_1] \times P[E_2] \quad [3]$$

Methodology of probabilistic approach

Probabilistic, risk-based methods have long been used, mainly in civil and other engineering disciplines. Examples of this can be found where probabilistic design methods are used almost routinely to assess the failure probability of building structures and rock slopes (Sjoberg[20]).

The general methodology of probabilistic approach assumes that the load (L) and the strength (S) of a structure can be described by two probability density functions, respectively, as shown in Figure 1. From Figure 1 it can be seen that the two curves overlap meaning that there exist values of strength which are lower than the load, thus implying that failure is possible in this overlap area. In a purely deterministic approach using only the mean strength and load, the resulting factor of safety would have been significantly larger than unity, which implies stable conditions.

To be able to calculate the probability that the load exceeds the strength, it is common to define a safety margin, SM, as

$$SM = S - L \quad [4]$$

The safety margin is one type of performance function which is used to determine the probability of failure. The performance function is often denoted $G(X)$, hence:

$$G(X) = S(X) - L(X) \quad [5]$$

where X is the collection of random input parameters which make up the strength and the load distribution, respectively. An alternative method to determine the performance function, which is often used in geomechanics, involves the factor of safety, F_S. Failure occurs when F_S is less than unity, hence the performance function is defined as (Sjoberg[20]):

$$G(X) = F_S - 1 \quad [6]$$

The probability density function (PDF) for the safety margin is illustrated in Figure 2. This Figure indicates that failure occurs when the safety margin is less than zero. The probability of failure (PoF) is the area under the density function curve for values less than zero, as shown in Figure 2.

The probability of failure is evaluated using a reliability index, β, defined in terms of the mean and the standard deviation of the trial factor of safety:

$$\beta = \frac{m_G - 1}{s_G} \quad [7]$$

where m_G and s_G are the mean and standard deviation of the performance function, respectively. The reliability index (RI) is a measure of the number of standard deviations separating the mean factor of safety from its defined failure value of 1.0, Figure 2 (Sjoberg[20]). It can also be considered as a way of

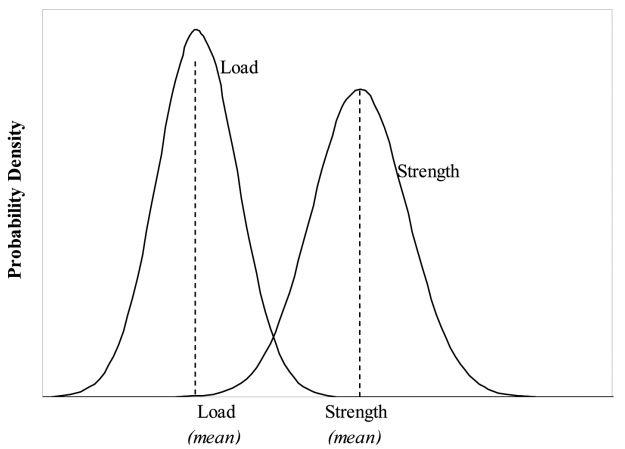

Figure 1—Hypothetical distribution of the strength and the load

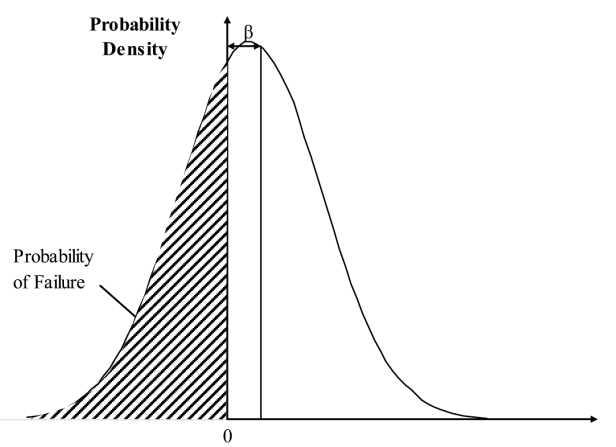

Figure 2—Hypothetical distribution of the safety margin, *SM*

normalizing the factor of safety with respect to its uncertainty. When the shape of the probability distribution is known, the reliability index can be related directly to the probability of failure.

Exact solutions for calculating the failure probability is possible only for simple cases. The performance function contains several variables describing the load and strength and is therefore often nonlinear, which prohibits exact analytical solutions (Sjoberg[20]). Commonly used approximate methods are:

- the first-order-second-moment method (FOSM) in which the performance function is approximated by a polynomial expansion into a linear expression
- the point estimate method (PEM), which is based on the precept that a probability distribution can be represented by point estimates (Rosenblueth[19]). This method is very simple for two to three variables and does not require extensive mathematical derivations; however, it becomes impractical for large numbers of input parameters.

The above methods are analytical means of determining the reliability index from a number of stochastic variables which make up the performance function. In cases where the performance function is complex and contains a large number of variables, a simulation technique can instead be used. The most common simulation technique is the Monte Carlo method. In this method, the distribution functions of each stochastic variable must be known. From each distribution, a parameter value is sampled randomly and the value of the performance function calculated for each set of random samples. If this is repeated a large number of times, a distribution of the performance function is obtained. The probability of failure can be calculated as the ratio between the number of cases which failed and the total number of simulations. Alternatively, the mean and standard deviation of the performance function distribution (factor of safety) can be calculated to yield the reliability index from which the failure probability can be determined using tabulated values for the standardized normal distribution (Sjoberg[20], Kim *et al.*[12]; Mostyn and Li[13]).

The Monte Carlo simulation is thus a procedure in which a deterministic problem is solved a large number of times to build a statistical distribution. However, Monte Carlo simulations can require substantial computer time. To overcome this, the more efficient Latin Hypercube sampling technique has been developed. In this method, stratified sampling is used to ensure that samples are obtained from the entire distribution of each input variable (Sjoberg[20]). This results in much fewer samples to produce the distribution of the performance function.

In general, the implementation of Monte Carlo method involves:

- Selection of a model that will produce a deterministic solution to a problem of interest
- Decisions about which input parameters are to be modelled probabilistically and the representation of their variabilities in terms of probability distributions
- Repeated estimation of input parameters that fit the appropriate probability distributions and are consistent with the known or estimated correlation between input parameters
- Repeated determination of output using the deterministic model
- Determination of the probability density function of the computed output.

Probabilistic analysis using the Monte Carlo simulation involves many trial runs. The more trial runs used in an analysis, the more accurate the statistics will be. The number of required Monte Carlo trials is dependent on the desired level of confidence in the solution as well as the number of variables being considered (Harr[10]), and can be estimated from:

$$N_{mc} = \left[\frac{d^2}{4(1-\varepsilon)^2} \right]^m \qquad [8]$$

where N_{mc} = number of Monte Carlo trials, d = the standard normal deviate corresponding to the level of confidence, ε = the desired level of confidence (0 to 100%) expressed in decimal form and m = number of variables.

The number of Monte Carlo trials increases geometrically with the level of confidence and the number of variables. For example, if the desired level of confidence is 90%, the normal standard deviate will be 2.71, the number of Monte Carlo trials will be 68 for one variable, 4 575 for two variables, and 309 445 for three variables. Theoretically, for a 100% level of confidence, an infinite number of trials would be required.

For practical purposes, the number of Monte Carlo trials is usually in the order of thousands. This may not correspond to a high level of confidence when multiple variables are being considered; however, the statistics computed from the Monte Carlo simulations are typically not very sensitive to the number of trials after a few thousands trials (Allen *et al.*[1]).

As mentioned above, fundamental to the Monte Carlo method is the process of explicitly representing the uncertainties by specifying inputs as probability distributions. By describing the process as a probability distribution, which has its origins in experimental/measurement continuous data, an outcome can be sampled from the probability distributions, simulating the actual physical process/measurement.

Goodness of fit test

In order to conduct a stochastic modelling, a collection of actual measurements and determining the best fits to the data using the goodness of fit tests (GOF) are required. GOF tests measure the compatibility of a random sample with a theoretical probability distribution function. Three most common GOF tests are:

- Kolmogorov-Smirnov
- Chi-square
- Anderson-Darling

The Kolmogorov-Smirnov test (Chakravarti *et al.*[7]) determines if two datasets differ significantly. An advantage of the Kolmogorov-Smirnov test is that the distribution of the test statistic itself does not depend on the underlying cumulative distribution function being tested. Another

advantage is that unlike the chi-square test, it is an exact test and does not require binned data and an adequate sample size for the approximations to be valid. Despite these advantages, the Kolmogorov-Smirnov test has several important limitations:

- It tends to be more sensitive near the centre of the distribution than at the tails
- The distribution must be fully specified. That is, if location, scale, and shape parameters are estimated from the data, the critical region of the Kolmogorov-Smirnov test is no longer valid. It typically must be determined by simulation.

The chi-square goodness of fit test (Snedecor and Cochran[21]) is used to test if a sample of data came from a population with a specific distribution (EasyFit©[9]).

An important feature of the chi-square test is that it can be applied to any distribution for which the cumulative density function can be calculated. The chi-square goodness-of-fit test can only be applied to binned data (i.e., data put into classes) and the value of the chi-square test statistic is dependent on how the data is binned. Another disadvantage of the chi-square test is that it requires a sufficient sample size in order for the chi-square approximation to be valid. The test requires that the data first be grouped. The actual number of observations in each group is compared to the expected number of observations and the test statistic is calculated as a function of this difference.

The Anderson-Darling test is a general test to compare the fit of an observed cumulative distribution function to an expected cumulative distribution function and can be applied to binned and unbinned data. It is a modification of the Kolmogorov-Smirnov test and is more sensitive to deviations in the tails of the distribution. The Anderson-Darling test makes use of the specific distribution in calculating critical values. This has the advantage of allowing a more sensitive test. The disadvantage of Anderson-Darling test is that the critical values must be calculated for each distribution.

The Anderson-Darling statistic (A^2) is defined as: (EasyFit©[9])

$$A^2 = -n - \frac{1}{n}\sum_{i=1}^{n}(2i-1)\left[\ln F(X_i) + \ln(1 - F(X_{n-1+i}))\right] \quad [9]$$

The hypothesis regarding the distributional form is rejected at the chosen significance level (α) if the test statistic, A^2, is greater than the critical value.

Acceptable probability of stability

Another important consideration in using the probabilistic approach is to use an acceptable PoF in the design. The acceptability of any given failure will depend on its consequence and perceived risk.

Vrijling and van Gelder[25] defined the following three kinds of limit states to construct a breakwater and recommended probability of failures depending on the failure characteristics:

- Ultimate limit states (ULS), describing immediate collapse of the structure.
- Serviceability limit states (SLS), describing loss of function of the structure without collapse
- Accidental limit states (ALS), describing failure under accident conditions (collision, explosions).

Vrijling and van Gelder[25] stated that usually low PoF is required for ULS compared to SLS and ALS in which the effects of failure are easily reversed.

Vrijling and van Gelder[25] developed the following classification and Table I to be used in the design of vertical breakwaters considering the probability of loss of life due to failure of the structure:

- Very low safety class, where failure implies no risk to human injury and very small environmental and economic consequences
- Low safety class, where failure implies no risk to human injury and some environmental and economic consequences
- Normal safety class, where failure implies risk to

Table I

Acceptance probability of failures for different safety class (after Vrijling and van Gelder[25])

Limit state type	Design probability of failure			
	Very low	Low	Normal	High
SLS / ALS	40%	20%	10%	5%
ULS	20%	10%	5%	1%

ALS Accidental limiting states
SLS Serviceability limiting states
ULS Ultimate limiting states

Table II

Acceptance criteria for rock slopes (after Priest and Brown[17], and Pine[15])

Category and consequences of failure	Example	Reliability index (β)	Probability of failure
1. Not serious	Non-critical benches	1.4	10%
2. Moderately serious	Semi-permanent slopes	2.3	1–2 %
3. Very serious	High/permanent slopes	3.2	0.3%

human injury and significant environmental pollution and high economic or political consequences

- High safety class, where failure implies risk to human injury and extensive environmental pollution and high economic or political consequences.

From Table I it is evident that even in ULS, 10 to 5 per cent probability is acceptable for low to normal safety classes.

The probabilities used in the design of open cast slopes are discussed by Priest and Brown[17] and Pine[15] who defined acceptance criteria according to Table II.

This Table indicates that for benches, probability of failure of around 10 per cent is accepted, whereas for an overall slope, a failure probability of less than 1 per cent would be more suitable.

A design criteria based on probability of failure is also recommended for Western Australian open cast mines, Table III. These design criteria have been developed from a combination of Department of Minerals and Energy's assessment of open cast mines in Western Australia[8] and a selection of published literature.

Similarly, this Table suggests a probability of failure of 1 per cent as acceptable in important slopes. This decreases to 0.3 per cent in populated areas where the slopes are near public infrastructures.

Washington State Department of Transportation (WSDOT, 2006) suggested maximum design probabilities of failure for road and highway cuts, fills, and landslide repairs. The recommended maximum probability of failure for different risk categories is presented in Table IV.

Based on these previous experiences, the probabilistic design criteria presented in Table V is tentatively suggested for roof bolting system design. It should, however, be noted that a detailed risk analysis based on the exposure of people is required to develop a conclusive design criteria, which is not the aim of this paper. Therefore, it is recommended that this design criteria should be evaluated before being fully implemented in underground coal operations.

In many engineering disciplines, probabilistic design has advanced to the stage that virtually all designs and guidelines are based on probabilistic approaches. The development has not yet reached this point in the field of rock engineering. One of the reasons for this is the difficulty associated with describing a rock mass quantitatively and defining a model which describes both the strength and the load acting on rock. This requires knowledge of roof failure mechanisms and a model which describes how failure occurs. The following sections of this paper aim at developing a deterministic model of failure mechanisms and a load/strength relationship to be used to develop a probabilistic design methodology for coal mine roof support design.

Roof behaviour and failure mechanism

Observed roof behaviour

In order to develop a realistic roof behaviour model, underground measurement data collected over many years in South African collieries, as part of SIMRAC projects (COL328, COL609 and COL712) was analysed in detail. A total of 55 intersection and roadway measurements from depths of 32 m to 170 m situated in significantly different geotechnical environments were analysed in terms of height and

Table III

Examples of design criteria for open pit walls (after DME, Western Australia[8])

Wall class	Consequence of failure	Design probability of failure	Pit wall examples
1	Not serious	Not applicable within containment structures.	Walls (not carrying major infrastructure) where all potential failures can be contained
2	Moderately serious	10%	Walls not carrying major infrastructure.
3	Serious	1%	Walls carrying major mine infrastructure (e.g. treatment plant, ROM pad, tailings structures).
4	Very serious++	0.30%	Permanent pit walls near public infrastructure and adjoining leases.

+ Potential failures have been defined as those modes of pit wall failure that have a POF of greater than 10%.
++ Where a mutually acceptable agreement to allow mining cannot be made between the mining company and the 'owner' of the adjoining structure or plot of land. Note that a higher standard of geotechnical data is required for the design of category 3 and 4 slopes compared to category 1 and 2 slopes.

Table IV

Slope stability—probability of failure (after WSDOT, 2006)

Conditions	Probability of failure
Unacceptable in most cases	> 0.1
Temporary structures with no potential life loss and low repair cost	0.1
Slope of riverbank at docks, no alternative docks, pier shutdown threatens operations	0.01 to 0.02
Low consequences of failure, repairs when time permits, repair cost less than cost to go to lower PoF	0.01
Existing large cut on interstate highway	0.01 to 0.02
New large cut (i.e., to be constructed) on interstate highway	0.01 or less
Acceptable in most cases except if lives may be lost	0.001
Acceptable for all slopes	0.0001
Unnecessarily low	0.00001

Table V

Suggested design criteria for the roof support systems

Roof class	Consequence	Reliability index (β)	Design probability of failure	Example
1	Moderately serious	1.4	5%	Short-term requirement (< 1 year), personnel access partially restricted
2	Serious	2.3	1%	Medium-term requirement (1–5 years) personnel access partially restricted
3	Very serious	3.2	0.3%	Long-term requirement (> 5 years) no personnel access restrictions

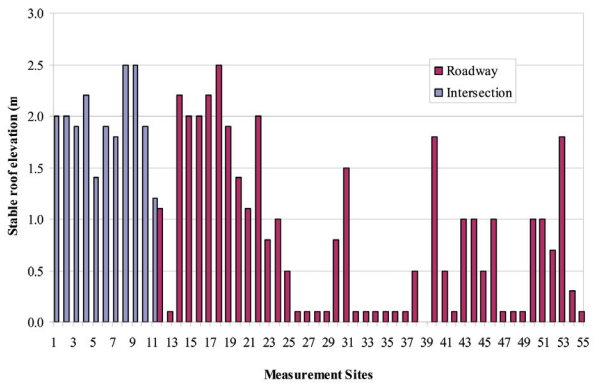

Figure 3—Measured height of roof-softening in intersections and roadways in South African collieries

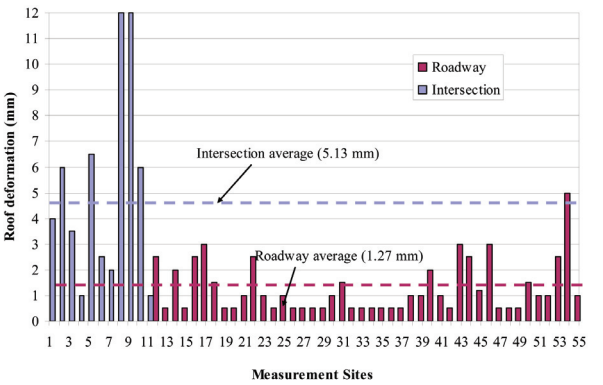

Figure 4—Measured deformations in intersections and roadways

magnitude of instabilities in the roof. The aim of this analysis was to:

- Establish at what heights the instabilities took place
- How these instabilities can be supported
- Establish a roof behaviour based on the magnitudes of deformations.

The results obtained from the height of instabilities are presented in Figure 3. This figure shows that the maximum measured height of instabilities in South African collieries is limited to 2.5 m into the roof, and there is no evidence of a substantial increase in the height of instabilities, as is the case in some overseas coal mines. This corresponds to a finding by van der Merwe *et al.*[24] that an insignificant number of roof falls in South African coal mines exceed 2 m in height.

Using the underground measurement data, a comparison was also made between the magnitude of deformations in intersections and roadways. The results indicated that, for a 41 per cent increase in the span (taken across the diagonal of an intersection) relative to the roadway span, the magnitude of the displacement in the roof increased by a factor of about four on average,

The magnitude of measured deformations is also evaluated against the maximum theoretical elastic deflection in a built-in beam using the following formula:

$$\eta_{\max} = \frac{\rho g L^4}{32 E t^2} \qquad [10]$$

where L = roof span (width of roadway)
t = thickness of roof layer (m)
ρ = density of suspended strata (kg/m^3)
g = gravitational acceleration (m/s^2)
E = Elastic modulus (Pa)

If the roof span (L) in the above formula increases by 41 per cent due to the diagonal width of the intersections, the deformation increases by a factor of 4.0. This is in accord with the findings in Figure 4.

In reality, intersections more closely resemble plates than beams, and one expression that has been suggested to analyse such plates is Equation [11],

$$\eta_{\max} = \frac{A \rho g L^4}{E t^2} \qquad [11]$$

where A is a constant that varies from 0.0138 to 0.0284 depending on the aspect ratio. However, Equation [10] is valid for a rectangular plate with clamped sides and there is no simple analytical solution for the intersection plate, i.e. a plate that is clamped on the four corners with free sides.

The above results obtained from the magnitudes of

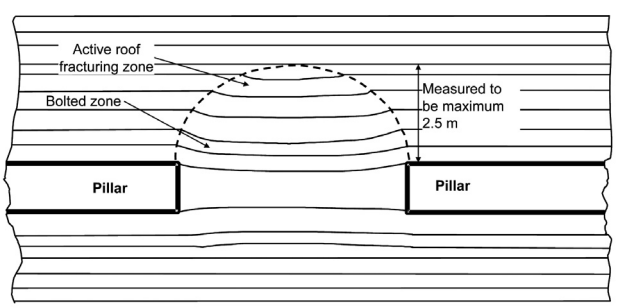

Figure 5—Zone of roof softening

deformations in intersections and roadways reveal that there is a significant correlation between the underground measurements and the beam theory. It is therefore concluded that the roof behaviour in South African collieries may be classified as similar to that of a clamped beam.

The results also suggest that based on the height of softening measurements, the suspension and beam building mechanisms (with improvements as discussed further in this paper) that have been used in South African collieries for many years are, in general, applicable where the appropriate conditions exist. It is, however, essential to determine the correct support mechanism to ensure the stability of roof.

From the results presented above, the roof behaviour model presented in Figure 5 is suggested.

This model suggests that when an underground opening is made, the portion of the strata directly above the opening loses its original support and the stress equilibrium is disturbed. The roof starts to sag under the gravitational and/or horizontal forces up to a height where there is a competent layer and a new equilibrium is reached. In the case of the absence of competent layers, as the lower layers start losing their integrity, the height of instabilities increase further into the roof. To maintain the stability, it is essential to keep the immediate, softened zone stable (Figure 5) using either suspension or the beam building mechanism. In the beam building mechanism, roof bolts in this zone force all the bolted layers to sag with the same magnitude; the layers within the bolting range thus act like a solid beam supporting the bolted horizon as well as the surcharge load due to softened layers higher into the roof.

Failure and support mechanisms

As indicated in the above model, before a roof bolt system is designed for a certain support mechanism, it is important to establish the geology for at least 2.5 m into the roof which will assist in identifying the expected roof behaviour and in determining the support mechanism to be used.

If the immediate roof is very weak, but a competent layer exits higher in the roof, the suspension support mechanism is indicated. However, when the entire roof consists of a succession of thin beams, none of which are self-supporting, the suspension principle cannot be applied and in this case the beam building mechanism is suggested.

It is suggested that before any decision has been made about the support system, a detailed geotechnical investigation should be conducted (especially in greenfield studies) to determine the heights of roof softening, which can be assumed to be extended up to the 'poor' quality layers (Canbulat and Van der Merwe[4]). This investigation can be carried out using the standard laboratory tests, impact splitting tests, RQD or rock mass rating.

In the suspension mechanism, the lower (loose) layer is suspended from the upper (competent) layer using roof bolts (Van der Merwe and Madden[23]). This creates a surcharge load and increases the maximum tensile stress in the upper layer, above the abutments. This surcharged tensile stress ($\sigma_{xx(\max)}$ in Pa) can be calculated using the following formula:

$$\sigma_{xx(\max)} = \frac{\rho g(t_{com} + t_{lam})L^2}{2t_{com}^2} \qquad [12]$$

where, ρ = density of suspended strata (kg/m^3)
g = gravitational acceleration (m/s^2)
L = span (bord width or intersectional diagonal width) (m)
t_{com} = competent layer thickness (m)
t_{lam} = laminated lower strata thickness (m)

For failure to take place, the tensile strength of the competent layer should be greater than the tensile stress generated in this layer due to surcharge load.

It should be noted that as mentioned above, the thickness of the competent layer, the position of the competent layer, the bord widths, the thickness of suspended strata and the strength of the competent layer will vary in nature. It is therefore suggested in determination of the applicability of the suspension mechanism using Equation [11] that a minimum of probability of stability of (PoS) 99 per cent should be attained.

The failure of rock under tension is invariably abrupt with total loss of cohesion and load carrying ability. Direct determination of tensile strength for rock, i.e. 'pull tests', is difficult, mainly because of involved specimen preparation. Indirect methods are most commonly used for determining the tensile strength.

The Brazilian (disc) method has proven to be a useful technique for a wide range of rock materials. It has, however, been found that the tensile strength determined by Brazilian tests is usually higher than the direct pull test value.

In general, while the rock material may have a tensile strength, a rock mass is often assumed to have very low tensile strength. This assumption is considered appropriate given the existence of joints and other defects in the rock mass. It is suggested that a detailed analysis should be conducted in determining the tensile strength of coal measure rock.

Roof bolting mechanisms

Suspension mechanism

The suspension mechanism is the most easily understood roof bolting mechanism. While the majority of roof bolts used are resin anchors, mechanical anchors are also uncommonly used (2 per cent only, Henson[11]).

The design of roof bolt systems based on the suspension principle has to satisfy the following requirements:

- The strength of the roof bolts has to be greater than the relative weight of the loose roof layer that has to be carried
- The anchorage forces of the roof bolts have to be greater than the weight of the loose roof layer.

The safety factor (SF_{sus}) of a bolting system in suspension mechanism is given by:

$$SF_{sus} = \frac{nP_f}{\rho g t_{lam}} \qquad [13]$$

where, ρ = density of suspended strata (kg/m3)
g = gravitational acceleration (m/s2)
P_f = resistance of a single bolt calculated from SEPT (kN)
t_{lam} = thickness of loose layer or layers (m)
n = number of bolts/m2

n can be calculated as follows:

$$n = \frac{k}{Ld} \qquad [14]$$

where d = distance between the rows of roof bolts (m)
L = span (bord width) (m)
k = number of bolts in a row

Beam building mechanism

Classical beam theory was first used by Obert and Duvall[14] in the design of roof bolt patterns. However, the derivations in this paper are taken directly from a standard reference (Popov[16]) to establish an improved design methodology for the beam building mechanism, which takes into account, where appropriate, the surcharge load (assumed to be parabolic) generated by the softened section above the bolted horizon.

The first consideration in the design of beam building mechanism is to determine the minimum required thickness of the beam which will be stable from the tensile failure point of view.

The maximum tensile stress must be smaller than the tensile strength of the upper layer of the built beam with an appropriate PoS (99 per cent). The maximum tensile stress in a built-beam with a parabolic surcharge load can be calculated as:

$$\sigma_{xx}\left(\pm\frac{L}{2}\right) = \frac{2}{5}\frac{\rho g L^2}{h^2}(h+h_1) \qquad [15]$$

The tensile stress in the lower surface at mid-span of the built-beam is:

$$\sigma_{xx}(0) = \frac{9}{40}\frac{\rho g L^2}{h^2}(h+h_1) \qquad [16]$$

Beams are subjected to transverse loads which generate both bending moments $M(x)$ and shear forces $V(x)$ along the beam. The bending moments cause horizontal stresses, σ_{xx}, to arise through the depth of the beam, and the shear forces cause transverse shear-stress distributions $\tau_{xy} = \tau_{yx}$ through the beam cross section as shown in Figure 6.

An important consideration in beam theory is that the top and bottom surfaces of the beam are free of shear stress, and the shear stress distribution across the beam is parabolic. As a consequence of this, the maximum shear stress (at the neutral axis of the beam) is given by:

$$\tau_{\max}(x) = \frac{3V(x)}{2A} \qquad [17]$$

The shear force distribution $V(x)$ is zero at the centre of a symmetrically loaded beam, and rises to a maximum at the end where it equals ½ of the total load. If the composite beam thickness is taken to be equal to the bolt length h, and the surcharge is parabolically distributed with a maximum height $h + h_1$ (Figure 5 and Figure 7), then

$$V_{\max} = \frac{1}{3}\rho g(h+h_1)L \qquad [18]$$

And from Equation [17]:

$$\tau_{\max} = \frac{1}{2}\frac{\rho g}{h}(h+h_1)L \qquad [19]$$

where h = built beam thickness (m)

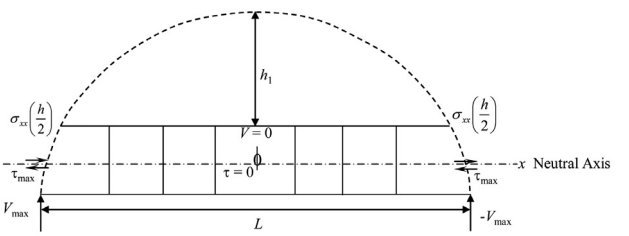

Figure 7—Computation and distribution of shear stress in a beam

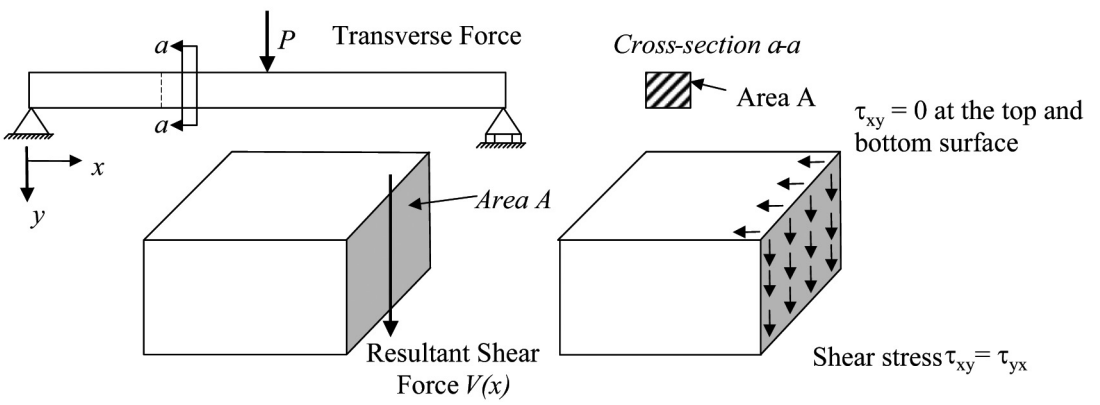

Figure 6—Beam with transverse shear force showing the transverse shear stress developed by it

Table VI

Results of shear box tests on various contacts typically found in coal mines

Number	Contact details	Friction angle (deg.)	Coefficient of friction
1	Coal/sandstone	23.6	0.44
2	Shale/sandstone	24.3	0.45
3	Coal/shale	24.8	0.46
4	Shale/sandstone	21.7	0.40
5	Shale/sandstone	24.7	0.46
6	Shale/sandstone	29.8	0.57
7	Coal/sandstone	25.8	0.48
8	Coal/sandstone	25.8	0.48
9	Sandstone/carbonaceous sandstone	24.3	0.45
10	Coal/shale	22.9	0.42
11	Sandstone/carbonaceous shale	25.1	0.47
12	Coal/carbonaceous shale	23.0	0.42
13	Sandstone/carbonaceous shale	20.2	0.37
14	Coal/coal	27.8	0.53
15	Coal/calcite	26.8	0.51
16	Sandstone/carbonaceous shale	22.7	0.42
17	Coal/sandstone	27.7	0.53
18	Coal/sandstone	25.1	0.47
19	Coal/laminated sandstone	25.2	0.47
Average		**24.8**	**0.46**
Standard deviation		**2.3**	**0.05**
Standard deviation as a percentage of average		**9.2**	**10.4**

h_1 = additional surcharge thickness (m)
L = span (m)
ρ = density of strata (kg/m^3)
g = gravitational acceleration (m/s^2)

For the built composite beam to act as a single entity, the shear stress given by Equation [19] has to be overcome by the action of the bolts. Two types of resistance are provided: frictional due to bolt pretensioning, and intrinsic shear strength of the bolts.

Neglecting the interlayer cohesion and layer deadweight, the frictional shear resistance of tensioned roof bolts can be calculated using the following well-known formula (Wagner[26]):

$$T_R = nF_p\mu \qquad [20]$$

where n is number of bolts per square meter, F_p is the pre-tension of bolt (usually 50 kN), and μ is the coefficient of friction between the layers.

In order to determine the coefficient of friction between the layers using shear box tests, a number of borehole samples from 5 collieries were obtained. Despite the variation in rock and contact types, the standard deviation of the friction angle is relatively low: 9.2 per cent of the average, Table VI. Note that the samples as tested may have been influenced by the drilling process. The influence of this has not been determined.

The shear strength of bolts also generates shear resistance, which must be considered in the design. This can be calculated using the following formula:

$$T_B = nS_R \qquad [21]$$

where S_R is shear strength of a bolt (in kN).

There have been extensive studies in the past to determine the shear strength of a bolt. In South Africa, it has previously been accepted that 50 per cent of the ultimate tensile strength (UTS) of a bolt is approximately equal to its shear strength (Wagner[26]). However, Azuar[2] concluded, from tests of resin-grouted bolts embedded in concrete, that the shear resistance of a joint when the bolt is installed perpendicular to the joint, is about of 90 per cent of the UTS.

Roberts[18] reported shear test results for smooth bars, rebars and cone bolts. He compared results of shearing an element at two interfaces (double shear) to a single interface shear and found that the former was not simply double the latter, as true symmetry did not exist in the case of double shear. Shear failure would occur at one interface first and subsequently resulted in failure of the other interface. From tests, he noted that a 16 mm diameter rebar had a static shear strength of approximately 90 per cent of the UTS.

Canbulat *et al.*[5], based on laboratory shear tests, also concluded that the shear strength of full-column roof bolts that are currently being used in South Africa is approximately 87 per cent of the ultimate tensile strength with very consistent results. Since this simple assumption will determine the required bolt length and density, it is suggested that the shear strength of a full column bolt is taken to be equal to 90 per cent of the UTS of a bolt.

Equation [21] then becomes:

$$T_B = 0.9nF_B \qquad [22]$$

where S_B is the ultimate tensile strength of a bolt (in kN).

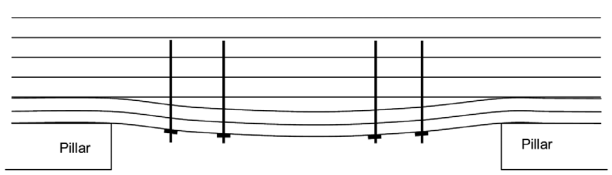

Figure 8—Bed separation within the bolted horizon

The shear resistance of a bolting system can therefore be determined as follows:

$$T_{TOTAL} = n(F_p\mu + 0.9S_B) \quad [23]$$

And for stability this has to exceed the value given by Equation [19].

$$SF = \frac{T_{TOTAL}}{\tau_{\max}} \quad [24]$$

Another important consideration in beam building mechanism occurs when the roof softening height is within the bolted horizon (Figure 8). This usually occurs when the bolts are installed late and the separation has already taken place and destroyed the cohesion between the layers or under excessive stress conditions.

In this case, safety factor (SF_{slide}) of resistance to sliding of the bolting system should be calculated using the bond strength (B_S) between the resin, rock and the bolt using the following formula:

$$SF_{slide} = \frac{kB_S l_{cap}}{Lt_{loose} d\rho g} \quad [25]$$

where
- B_S = bond strength or grip factor (kN/mm)
- d = distance between the rows of roof bolts (m)
- L = span (bord width) (m)
- t_{loose} = thickness of separated layer (m)
- k = number of bolts in a row
- l_{cap} = capsulation length (bolt length – t_{loose}) (m)
- ρ = density of strata (kg/m^3)
- g = gravitational acceleration (m/s^2)

Bond strength is measured through short encapsulation pull tests (SEPT). In order to measure the bond strength, it is necessary to shear the bond on the bolt-resin or resin-rock interface. With the modern high-strength, high-stiffness, polyester resins, it has been found that a bond length of 250 mm is appropriate for determining the bond strength.

Bond strength (B_S) is defined as:

$$B_S = \frac{Maximum\ \ load\ \ achieved\,(kN)}{Encapsulation\ \ length\,(mm)} \quad [26]$$

Similar to the suspension mechanism, to avoid the failure of roof bolts in tension, the safety factor (SF_{bolt}) of roof bolts should also be determined. The following formula can be used to calculate the safety factor of roof bolts:

$$SF_{slide} = \frac{kP_{bolt}}{Lt_{loose} d\rho g} \quad [27]$$

where
- P_{bolt} = bolt yield strength (kN)
- d = distance between the rows of roof bolts (m)
- L = span (bord width) (m)
- t_{loose} = thickness of separated layer (m)
- k = number of bolts in a row
- ρ = density of strata (kg/m^3)
- g = gravitational acceleration (m/s^2)

Probability density functions of design parameters and random selection

Available probability density functions

As indicated in the previous section, the fundamental to the Monte Carlo method is the process of explicitly representing the uncertainties by specifying inputs as probability distributions. Probability density functions are the tools used to estimate the likelihood that random variable values will occur within certain ranges. There are two types of random variables, namely discrete and continuous. A discrete (finite) random variable can take only a countable number of distinct values. A continuous (infinite) random variable can, however, take an unknown number of possible samples and the samples are not countable, but are taken from a continuous interval. Because few, if any, geotechnical properties will behave as a discrete probability space, discrete distributions are not presented.

The probability density function is a function that assigns a probability to every interval of the outcome set for continuous random variables. The probability density function is denoted $f_X(x)$, where x is the random variable itself and x is the value that the continuous random variable can take on. Probability functions have the following properties (Allen *et al.*[1]):

- The function is always nonnegative, $F_X(x) \geq 0$
- The area under the function is equal to one,

$$\int_{-\infty}^{\infty} f_x(x)dx = 1$$

- The probability that a random value, X, from the distribution is between a and b is

$$P[a \leq x \leq b] = \int_a^b f_x(x)dx \quad [28]$$

Cumulative probability distribution functions have the value at x_0 corresponding to the probability that a random value, X, from the distribution will be less than or equal to x_0.

For a continuous distribution, this can be expressed mathematically as

$$\Pr(X \leq x_0 = \int_{-\infty}^{x_0} f(x)\,dx \quad [29]$$

Over 25 special continuous probability density distributions exist. Only the following 9 most commonly used distributions are used in this paper:

- Beta
- Erlang
- Exponential
- Gamma
- Logistic
- Lognormal

Table VII

Summary of probability distributions (after EasyFit[9])

Distribution	Parameters	Density distribution function	Cumulative distribution function	Definitions
Beta	α_1 continuous shape α_2 continuous shape	$f(x)=\frac{x^{\alpha_1-1}(1-x)^{\alpha_2-1}}{B(\alpha_1,\alpha_2)}$	$F(x)=\frac{B_x(\alpha_1,\alpha_2)}{B_x(\alpha_1,\alpha_2)}\equiv I_x(\alpha_1,\alpha_2)$	B = Beta function B_x = Incomplete beta function
Erlang	m integral shape β continuous scale	$f(x)=\frac{1}{\beta(m-1)!}\left(\frac{x}{\beta}\right)^{m-1}e^{-x/\beta}$	$F(x)=\frac{\Gamma_{x/\beta}(m)}{\Gamma(m)}=1-e^{-x/\beta}\sum\frac{(x/\beta)^i}{i!}$	Γ = Gamma function Γ_x = Incomplete gamma function
Exponential	β continuous scale	$f(x)=\frac{e^{-x/\beta}}{\beta}$	$F(x)=1-e^{-x/\beta}$	
Gamma	α continuous shape β continuous scale	$f(x)=\frac{1}{B\Gamma(x)}\left(\frac{x}{\beta}\right)^{\alpha-1}e^{-x/\beta}$	$F(x)=\frac{\Gamma_{x/\beta}(\alpha)}{\Gamma(\alpha)}$	Γ = Gamma function Γ_x = Incomplete gamma function
Logistic	α continuous location β continuous scale	$f(x)=\frac{\sec h^2\left[\frac{1}{2}\left(\frac{x-\alpha}{\beta}\right)\right]}{4\beta}$	$F(x)=\frac{1+\tan h\left[\frac{1}{2}\left(\frac{x-\alpha}{\beta}\right)\right]}{2}$	*sec h* = hyperbolic Secant Function *tan h* = hyperbolic Tangent Function
Lognormal	μ continuous σ continuous	$f(x)=\frac{1}{x\sqrt{2\pi}\sigma'}e^{-\frac{1}{2}\left[\frac{\ln x-\mu'}{\sigma'}\right]^2}$	$F(x)=\Phi\left(\frac{\ln x-\mu'}{\sigma'}\right)$	$\mu'\equiv\ln\left[\frac{\mu^2}{\sqrt{\sigma^2+\mu^2}}\right]$ $\sigma'\equiv\sqrt{\ln\left[1+\left(\frac{\sigma}{\mu}\right)^2\right]}$ $\Phi(z)$ = Laplace-Gauss integral
Normal	α continuous location β continuous scale	$f(x)=\frac{1}{\sqrt{2\pi}\sigma'}e^{-\frac{1}{2}\left[\frac{x-\mu}{\sigma}\right]^2}$	$F(x)=\Phi\left(\frac{\ln x-\mu}{\sigma}\right)=\frac{1}{2}\left[erf\left(\frac{x-\mu}{\sqrt{2}\sigma}\right)+1\right]$	Φ = Laplace-Gauss integral *erf* = error function
Pert	$\mu\equiv\frac{\min+4\,m..likely+\max}{6}$ $\alpha_1\equiv 6\left[\frac{\mu-\min}{\max-\min}\right]$	$f(x)=\frac{(x-\min)^{\alpha_1-1}(\max-x)^{\alpha_2-1}}{B(\alpha_1,\alpha_2)(\max-\min)^{\alpha_1+\alpha_2-1}}$	$F(x)=\frac{B_z(\alpha_1,\alpha_2)}{B(\alpha_1,\alpha_2)}\equiv \mathrm{I}_z(\alpha_1,\alpha_2)$	min = continuous boundary parameter (min < max) m.likely = continuous parameter (min<m.likely<max) max = continuous parameter $z\equiv\frac{x-\min}{\max-\min}$
	$\alpha_2\equiv 6\left[\frac{\max-\mu}{\max-\min}\right]$			B = Beta function B_z = Incomplete beta function
Weibull	α continuous shape β continuous scale	$f(x)=\frac{\alpha x^{\alpha-1}}{\beta^\alpha}e^{-(x/\beta)^\alpha}$	$F(x)=1-e^{-(x/\beta)^\alpha}$	

Table VIII

Summary results of Anderson-Darling goodness of fit tests

Parameter	Number of data points	Best fit probability distribution	Scale parameter	Shape parameter	Location parameter
Bord width (m)	258	Logistic	0.32	N/A	6.23
Distance between the bolts (m)	835	Pert	1.90 (mode)	0.58 (min)	3.31 (max)
Pretension of roof bolts (kN)	122	Pert	29.80 (mode)	18.92 (min)	82.50 (max)
Height of roof softening (m)	93	Logistic	0.17	N/A	0.65
Unit weight (MN/m^3)	168	Erlang	16.24	148	N/A
Bond strength (kN/mm)	46	Lognormal	0.29	N/A	-0.87
Coefficient friction (^{o})	19	Lognormal	0.1	N/A	-0.78
Bolt strength (kN)	192	Logistic	0.36	N/A	120.4
Tensile strength of sandstone (MPa)	30	Pert	3.15 (mode)	0.46 (min)	5.19 (max)
Tensile strength of weak rock (MPa)	66	Pert	0.79 (mode)	0.32(min)	3.44 (max)
Thickness of competent layer (m)	43	Weibull	2.6	2.84	N/A
Thickness of suspended layer (m)	43	Normal	0.2	N/A	0.89

- Normal
- Pert
- Weibull

Rather than focus on the derivations, useful properties of these distributions are presented in Table VII.

In order to determine the best fit probability density distributions for each of the input parameters used in the design, the underground measurement data collected throughout this study has been analysed using the Anderson-Darling goodness of fit test.

Probability distributions of design parameters

Based on the load/strength models presented in earlier, the following parameters' probability distributions will be determined to use in the probabilistic design of roof bolting systems:

- Bord width
- Distance between the bolts (in determining the roof bolt density)
- Pretension of roof bolts
- Height of roof softening
- Unit weight
- Bond strength
- Coefficient friction
- Bolt strength
- Tensile strength of rock
- Thickness of competent layer
- Thickness of suspended layer

Note that the distribution of roof bolt strength is calculated from the variation in the diameter of 18 mm roof bolts using a constant ultimate steel strength of 600 MPa.

A summary of the goodness of fit test results using the Anderson Darling test is summarized in Table VIII.

Note that, as can be seen, the results presented in Table VIII are based on a limited number of data points. Therefore, certain best fit probability distributions obtained from Anderson-Darling goodness of fit tests are only marginally better than the others, such as Weibull distribution is only slightly better than the normal distribution for the thickness of the competent layer. This indicates that a more comprehensive database is required to establish the conclusive distributions of design parameters.

Support design methodology

Using all above, the following step-by-step process is suggested in the design of a roof support system:

1. Conduct a detailed geotechnical analysis to determine the height of roof softening and distribution of input parameters. This can be achieved for existing operations from underground measurements and/or height of FOG, and for greenfield studies it can be estimated using existing geotechnical rating systems.
2. Determine the applicability of the suspension mechanism using Equation [11]. Note that a minimum PoS of 99 per cent is recommended to use the suspension mechanism with confidence.
3. Further detailed geotechnical analyses are required to determine the distributions of suspension and beam building mechanisms' input parameters.
4. Conduct short encapsulated pull tests to calculate the support resistance.
5. For the appropriate support mechanism calculate the probability of stabilities of different length of roof bolts. Note that if required a sensitivity analysis into the distance between the rows of support elements, bord width, bond strength and pretension on roof bolts can be conducted at this stage.
6. Check the probability of stabilities achieved against the design criteria given in Table V. If the design criteria is not achieved go back to Step 4.
7. If the design criteria is achieved in Step 6, check the stability between the roof bolts.
8. Determine the financial viability of the system. If the system is financially viable, implement it; otherwise conduct a detailed analysis into different bolting systems in Step 5.
9. Once the bolting system is implemented (i) monitor the support system and (ii) implement the appropriate quality control procedures.

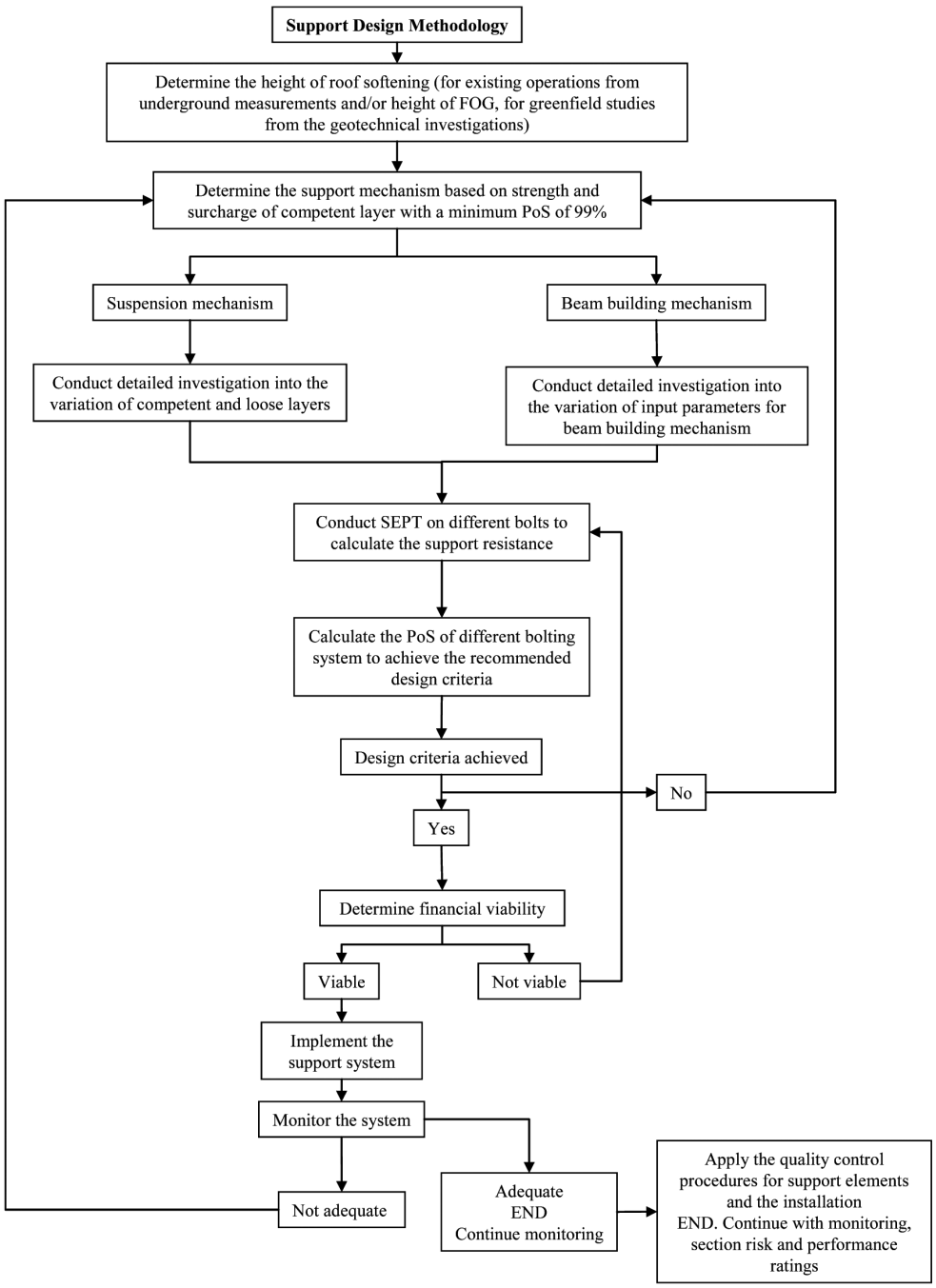

Figure 9—Recommended support design methodology

10. As an on going procedure, use appropriate (developed for the specific conditions) section performance and risk rating system and continue monitoring the support system and the roof behaviour.

A design flow-chart summarizing the above methodology is presented in Figure 9.

Application of the probabilistic design approach to a case study

In the previous sections, a probabilistic design methodology is presented. In this section a verification of this design methodology will be demonstrated by applying it to a well-defined study with the aim of establishing the best support system for a colliery situated in the Witbank Coalfield.

Description of input data

A detailed monitoring program was conducted in a bord and pillar section of Colliery 'A'. Using three sonic probe monitoring sites (two in roadways and one in an intersection) the roof behaviour was monitored and the height of roof softening data was obtained. The mine experienced roof falls for a period of time and an investigation into the thickness of roof falls was therefore

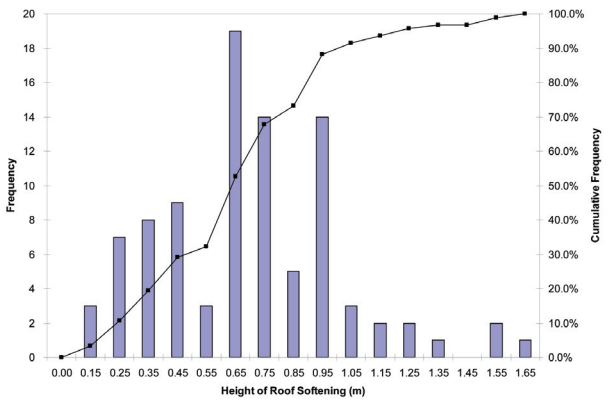

Figure 10—Colliery 'A' height of softening data obtained from the sonic probe extensometer results, feeler-gauge results and FOG data

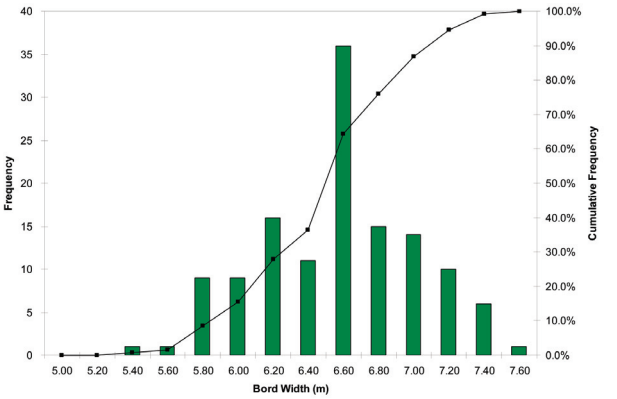

Figure 11—Bord width distributions in the experiment site

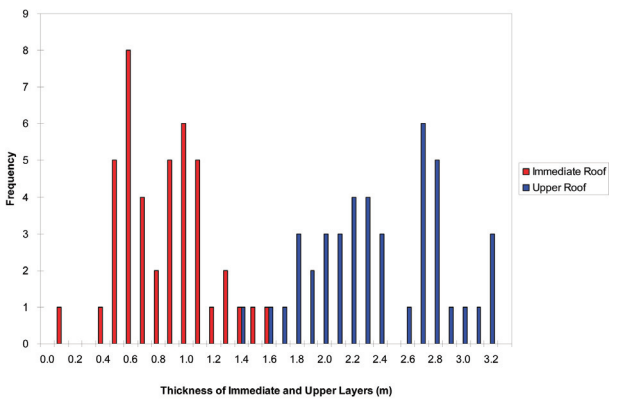

Figure 12—Thickness of immediate and upper roof obtained from borehole logs

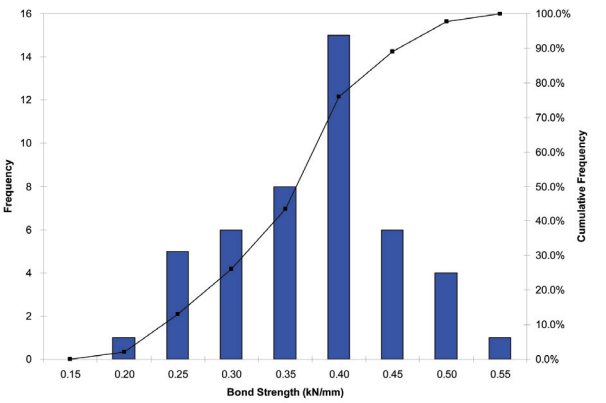

Figure 13—Bond strength results obtained from SEPT in the experiment site

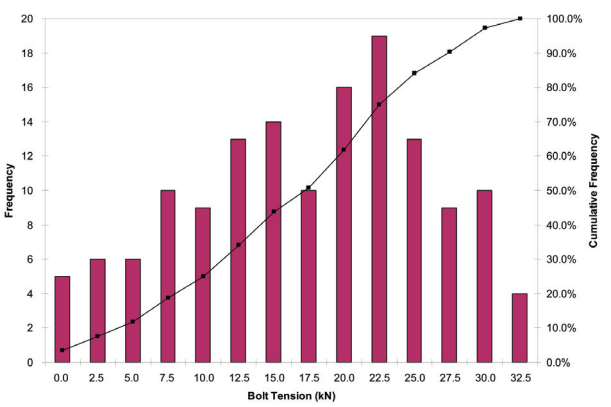

Figure 14—Distribution of roof bolting tensioning results

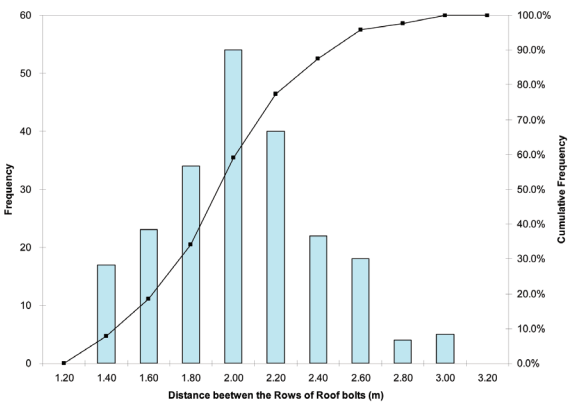

Figure 15—Distance between the roof bolts measured in the experiment site

conducted. This data was also combined with the sonic probe data to extend the height of roof softening database. Figure 10 summarizes the data obtained from these three different techniques. It is evident from this Figure that the height of softening varies from 0.15 m to 1.65 m with an average of 0.65 m.

A detailed bord width measurement programme was also conducted and bord width offsets were measured in two different production sections. A frequency versus bord width graph is given in Figure 11. In these two sections, the bord widths were designed to be 6.5 m, but, in reality varied from 5.4 m to 7.6 m.

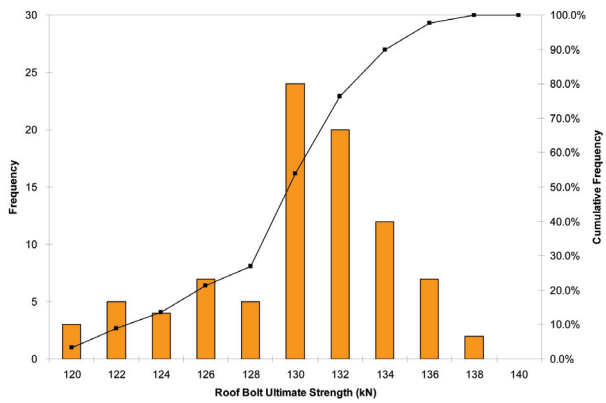

Figure 16—Roof bolt ultimate strength

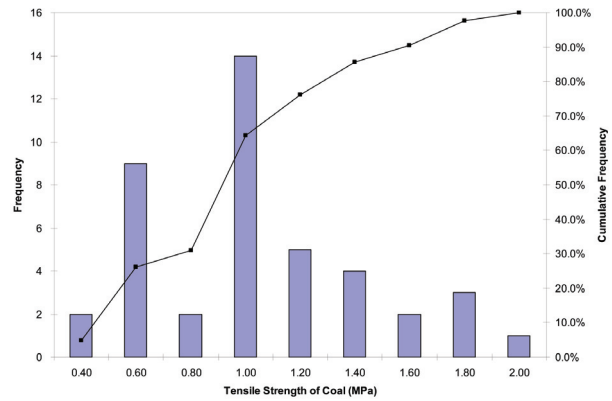

Figure 17—Distribution of tensile strength of coal used in the analysis

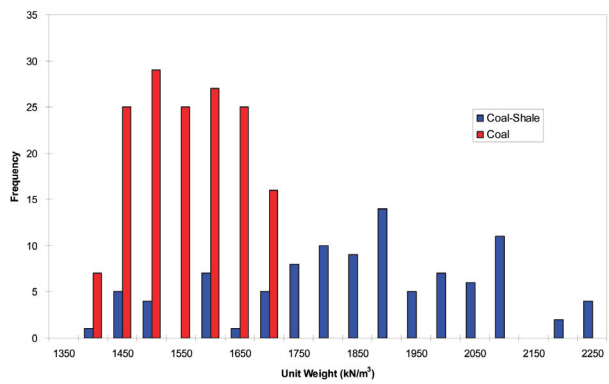

Figure 18—Unit weights of the immediate and upper coal layers

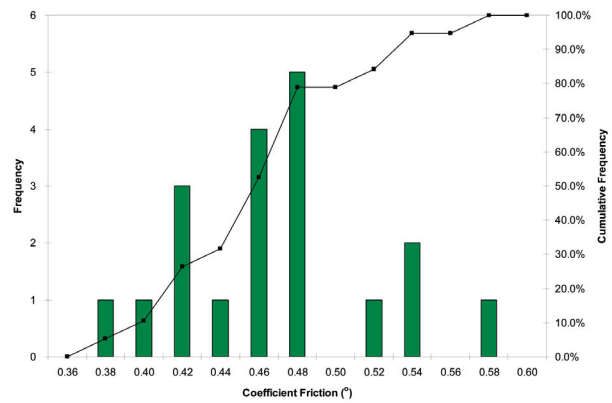

Figure 19—Distribution of coefficient of friction between the layers

Table IX

Summary of information used in the analysis

	Number of samples	Minimum	Maximum	Average	Mode
Height of roof softening (m)	93	0.2	1.6	0.7	0.6
Bord widths (m)	129	5.3	7.5	6.5	6.5
Thickness of immediate layer (m)	43	0.1	1.6	0.8	1
Thickness of upper coal layer (m)	43	1.5	3.3	2.5	2.1
Bond strength (kN/mm)	46	0.2	0.6	0.4	0.4
Bolt tensioning (kN)	145	0	32	16.4	20
Distance between the rows of roof bolts (m)	217	1.3	3	2	2
Roof bolt ultimate strength (KN)	209	119.3	137.8	129.3	126
Unit weight of immediate layer (MN/m3)	99	1382.8	2214.4	1835.3	1900
Unit weight of upper coal layer (MN/m3)	154	1380.9	1669.7	1530.1	1531.2
Coal tensile strength (MPa)	40	0.4	1.8	1	1.2
Coefficient of friction between the layers (°)	19	0.4	0.6	0.5	0.4
Coalfield	Witbank				
Seam	No. 2				
Mining height	3.0 m				
Mining method	Continuous miner bord and pillar, 9 road section				
Depth	47 m				
Pillar widths	9.0 m				
Cut out distance	8.0 m				

The immediate roof strata consisted of 0.1 to 1.0 m of coal, followed by a shale band approximately 0.3 m thick above which there is a further 3.0 m of coal. This data were obtained from the borehole logs that were available at the mine where the bord width measurements and the height of roof softening data were collected. Figure 12 illustrates the distributions of thicknesses of the immediate and the upper roof coal layers. In this Figure, the immediate roof thicknesses included the skin coal and the shale band whereas the upper roof included the coal thickness overlying the immediate roof.

A series of underground short encapsulation pull tests

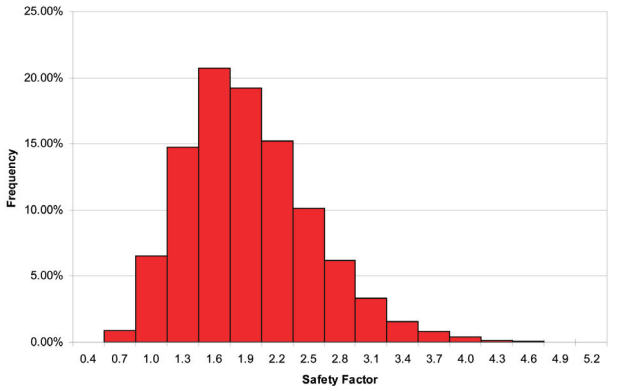

Figure 20—Distribution of safety factors of upper coal layer in suspension mechanism

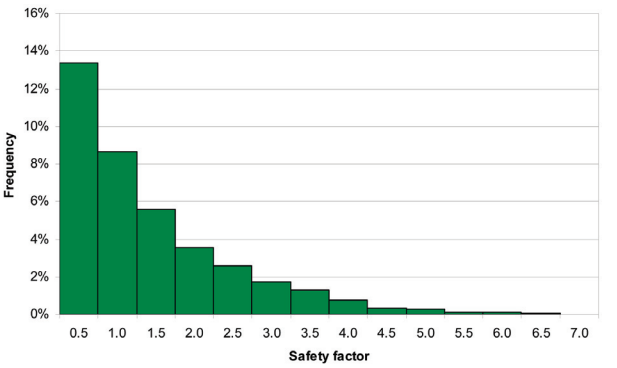

Figure 21—Distribution of safety factors in suspension mechanism using 1.2 m long roof bolts

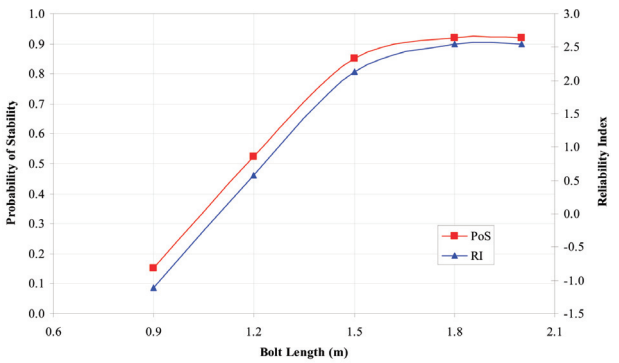

Figure 22—PoS and Reliability Index for suspension mechanisms for different roof bolt lengths

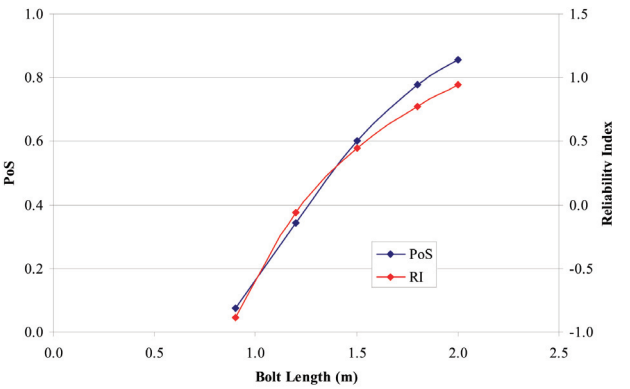

Figure 23—Probability of stability and reliability index of different length roof bolts, 3 roof bolts in a row

were carried out in near identical conditions in those two sections. Tests were performed using the 30 second spin and hold resin and 1.2 m long, 16 mm roof bolts, as currently being used by the mine, Figure 13. Note that due to the time laps between the tests and the need for the roofbolter in production schedule, tests were conducted in different areas of the sections.

In order to determine the tension on the roof bolts, over 145 roof bolts were tested using a torque-wrench. Figure 14 shows the distribution obtained from these measurements. As can be seen the tension on the roof bolts varied from 0 to 32.5 kN.

Distances between the rows of roof bolts were also measured in the monitoring site, Figure 15. Similar to bord widths, although the planned distance was 2.0 m, in reality it varied from 1.4 m to 3.2 m.

In order to determine the strength of roof bolts based on a constant 600 MPa ultimate steel strength, bolt diameter measurements were also taken over 80 bolts at the mine and the ultimate strength of roof bolts were determined, Figure 16.

A laboratory testing programme was also initiated to determine the tensile strength of the immediate and upper coal layers with the aim of determining the applicability of suspension and beam building mechanisms as well as the stability of the immediate roof between the roof bolts. Additional information such as the unit weights of coal and shale was also determined from these laboratory tests. The distribution of tensile strength of coal as obtained from the Brazilian tensile strength tests is shown in Figure 17. Figure 18 shows the distribution of unit weights of the immediate and the upper coal layers determined from these laboratory tests.

Due to the lack of information at the mine about the coefficient of friction between the layers in the roof, the data presented in Table VI were used in this study. Figure 19 illustrates the distribution of the data given in Table VI.

A summary of the information presented above is given in Table IX together with the additional information obtained from the mine.

Results

In order to determine the support mechanism using the above input parameters, the applicability of the suspension mechanism, as applied by the mine, was investigated. A total of 20 000 Monte Carlo simulations were run using Equation [11] and the results showed that although the average safety factor of the upper coal layer is 1.79, the PoS by using the

Table X

Stability analyses of different support patterns

Support pattern		Bolt length (m)				
		0.9 m	1.2 m	1.5 m	1.8 m	2.0 m
4 bolts in a row 2.0 m spacing between the rows	Probability of stability	0.113	0.642	0.907	0.981	0.994
	Reliability index	-0.834	0.461	1.238	1.756	2.015
5 bolts in a row 2.0 m spacing between the rows	Probability of stability	0.348	0.895	0.989	0.999	1.000
	Reliability index	0.203	1.233	1.852	2.264	2.470
4 bolts in a row 1.5 m spacing between the rows	Probability of stability	0.435	0.959	0.999	1.000	1.000
	Reliability index	0.498	1.784	2.556	3.070	3.328
5 bolts in a row 1.5 m spacing between the rows	Probability of stability	0.644	0.990	1.000	1.000	1.000
	Reliability index	1.549	2.594	3.222	3.640	3.849

suspension mechanism is only 92.6 per cent with a Reliability Index of 0.53, which is not acceptable according to the requirements (i.e., the minimum required PoS should be 99 per cent). Figure 20 presents the distribution of safety factors for the stability of the upper coal layer using the probability distributions presented in Table VIII.

The results further showed that the overall PoS by using the suspension mechanism (PoS of upper component layer × PoS of bolts × PoS of sliding of roof bolts) is only 52 per cent (see Figure 21 for the distribution of safety factors in the suspension mechanism). In other words, 48 per cent of the roof supported using the suspension mechanism with 1.2 m roof bolts would be expected to result in failure.

Figure 22 shows the probability of stabilities and the reliability indices for different lengths of roof bolts in the suspension mechanism. As can be seen from this Figure, the maximum PoS that can be achieved is 92 per cent even when using 2.0 m long roof bolts, which still does not meet the design criteria. Note that since the PoS of the suspension mechanism is dependent on the PoS of the upper coal layer, the maximum PoS that can be achieved for the suspension mechanism is limited to 92.6 per cent.

From these analyses it is evident that the suspension mechanism, as it is currently used by the mine, is not the correct support mechanism for the roof conditions present at the mine. Therefore, beam building mechanism using full-column resin bolts is indicated and a further study into the design of a roof bolting system using the beam building mechanism was conducted.

As a preliminary study, the mine's current support pattern, three bolts in a row with 2.0 m spacing was evaluated for the beam building mechanism by assuming that the bolts are full-column resin bonded. The probabilities of stability and the reliability indices for different roof bolts lengths achieved from this study is presented in Figure 23. From this Figure it is evident that the current pattern used by the mine is not sufficient to achieve the required probability of stability even though the bolts are full-column resin bonded. Note that the overall probabilities of stability that are presented in Figure 23 include the probability of stability of shear loading, the probability of bolt sliding and the probability of bolt tension failures.

Table X shows the probabilities of stability and the reliability indices achieved for 16 mm, 4 and 5 roof bolt patterns using 2.0 m and 1.5 m row spacing. From this Table, the following minimum support patterns are recommended for different risk category areas:

- In moderately risk category areas:
  - Four 1.8 m long roof bolts, 2.0 m row spacing
  - Five 1.5 m long roof bolts, 2.0 m row spacing
- In serious risk category areas:
  - Five 1.8 m long roof bolts, 2.0 m row spacing
  - Four 1.5 m long roof bolts, 1.5 m row spacing
- In very serious risk category areas:
  - Five 1.5 m long roof bolts, 1.5 m row spacing.

An important consideration at this stage is to conduct a simple cost analysis for different roof bolt systems to determine the financial viability of each system. Once the bolting system is chosen and implemented, it is important that the support system should continuously be monitored and appropriate quality control procedures should be implemented.

Conclusions

The ultimate aim of this study was to develop a roof support design methodology that takes into account natural variations that exist within the rock mass and the mining process. This was achieved by adopting a probabilistic design approach using the well established stochastic modelling technique, which is widely used in civil and other engineering disciplines.

In the literature, it has been highlighted that some of the disadvantages of the probabilistic approach are the various assumptions about the distribution functions. This limitation has been overcome by using the actual data obtained during this study. The probability distributions of various input parameters were established using the Anderson-Darling goodness of fit tests.

It is shown that the traditional deterministic roof bolt design methodologies provide some insight into the underlying mechanisms, but they are not well suited to making predictions as input into roof support decision-making as they cannot quantitatively address the risks and uncertainties that are inherently present.

Analysis of the underground monitoring data revealed that there is good correlation between the underground measurements and predictions based on simple beam theory, which has been used in the design of roof support systems for many years in South Africa. The design methods used are thus fundamentally sound, but incomplete as they do not explicitly account for variability. Therefore, in the development of the probabilistic approach, the deterministic approaches used in South Africa have been improved, especially the beam building mechanism.

The design approach was applied to a well-defined case study in a colliery in the Witbank Coalfield, where the variations of all parameters that impact the roof and support behaviours were evident. The suspension mechanism has historically been used in this mine, which resulted in roof falls. It has been shown using the input parameters collected from the mine that the suspension mechanism is not suitable for the conditions present. The probabilistic methodology described in the paper was then further used to analyse different support configurations using the beam building mechanism and suitable configurations were found. Therefore, the beam building mechanism was recommended for different risk category areas using four or five roof bolts with different lengths and row spacings.

In essence, the improvement in expected stability was obtained by using the existing support design philosophies (i.e. suspension and beam building), but by adopting a probabilistic approach rather than the currently used deterministic approach.

References

1. Allen L.J., Kramer, S.L. and Arduino, P. *Estimation of uncertainty in geotechnical properties for performance-based earthquake engineering*. Pacific Earthquake Engineering Research Center. College of Engineering. University of California, Berkeley. 2002.
2. Azuar J.J. Stability of fractured rock masses by sealed steel bar. L.C.P.C. *Rapport de recherche LPC* No. 73 (in French), Nov. 1977.
3. Canbulat, I. and Jack, B.W. Review of current design methodologies to improve the safety of roof support systems, particularly in the face area, in collieries. Safety in Mines Research Advisory Committee (SIMRAC). Final Project Report, COL 328. 1998. 212 pp.
4. Canbulat, I. and van der Merwe, J.N. Extended cut-out distances in continuous miner sections in South African collieries. S.S. Peng (ed.) *Proceedings of the 19th International Conference on Ground Control in Mining*. Morgantown, WV: 2000. pp. 325–331.
5. Canbulat, I., Wilkinson, A. and Prohaska, G.P. Optimisation of Support in Collieries (a continuation of SIM020205). SIMRAC, Department of Minerals and Energy, Johannesburg, South Africa Final Project Report SIM 020205b. March. 2006.
6. Canbulat, I., Wilkinson, A. and Prohaska, G.P. An investigation into the support systems in South African collieries. SIMRAC, Department of Minerals and Energy, Johannesburg, South Africa Final Project Report SIM 020205. March. 2005.
7. Chakravarti, I.M., Laha, R.G. and Roy, J. *Handbook of methods of applied statistics*, Volume I, John Wiley and Sons, 1967. pp. 392–394.
8. Department of Minerals and Energy, Western Australia. Geotechnical considerations in open pit mines. Guideline. August, 1992.
9. EasyFit©. User Manual. MathWave Version 3. http://mathwave.com. 2006.
10. Harr, M.E. *Reliability-based design in Civil Engineering*. McGraw-Hill Inc. 1987.
11. Henson, N. World wide statistics, roof support. SANIRE Coalfields Branch technical presentation. SA Coal Estates Colliery, Witbank. December. 2005.
12. Kim, H.S., Majr, G. and Ross-Brown, D.M. Application of Monte Carlo techniques to slope stability analyses. *Preprint-Proceedings 19th US Symposium on Rock Mechanics*. Stateline, Nevada, 1978. pp. 28–39.
13. Mostyn, G.R. and Li, K.S. Probabilistic slope analysis—State-of-play. *Probabilistic Methods in Geotechnical Engineering, Proc*. Canberra, February 10–12, 1993. pp. 89–109. Rotterdam: A. A. Balkema.
14. Obert, L. and Duvall, W. I. *Rock mechanics and the design of structures in Rock*. John Wiley and Sons, USA, 1967.
15. Pine, R.J. Risk analysis design applications in mining geomechanics. *Trans. Instn. Mine. Metall.* (Sec. A: Min. Industry), vol. 1001, 1992. pp. A149–158.
16. Popov, E.P. *Mechanics of materials*. 2nd Edition. Prentice/Hall International, Inc. Englewood Cliffs, New Jersey. 1978.
17. Priest, S.D. and Brown, E.T. Probabilistic stability analysis of variable rock slopes. *Trans. Instn. Min. Metall.* (Sect. A: Min. Industry), vol. 92, 1983. pp. A1–A12.
18. Roberts, D.P. Testing of mining tunnel support elements and systems for hard rock mines, Master of Science in Engineering to the Department of Mechanical Engineering, University of Natal, South Africa. 1995.
19. Rosenblueth, E. Point estimates for probability moment. *In Proc. Nat. Acad. Sci. USA*, vol. 72, no. 10, 1975. pp. 3812–3814.
20. Sjoberg, J. Large scale slope stability in open pit mining—a review. Technical Report. Lulea University of Technology, Division of Rock Mechanics. Report No: 1996:10T. 1996.
21. Snedecor, G.W. and Cochran, W.G. *Statistical methods*, Eighth Edition, Iowa State University Press. 1989.
22. Van der Merwe, J.N. A probabilistic approach to the design of coal mine roof support systems. Advances in rock mechanics in underground coal mining. *SANGORM Symposium*, September. 1989.
23. Van der Merwe, J.N. and Madden, B.J. *Rock engineering for coal mining*. Safety in Mines Research Advisory Committee (SIMRAC). SAIMM Special Publications Series 7. April 2002.
24. Van der Merwe, J.N., van Vuuren, J.J., Butcher, R. and Canbulat, I. Causes of falls of roof in South African collieries. SIMRAC, Department of Minerals and Energy, Johannesburg, South Africa Final Project Report, Report No: COL613. March 2001.
25. Vrijling J.K. and P.H.A.J.M. van Gelder. The effect of inherent uncertainty in time and space on the reliability of flood protection, *ESREL'98: European Safety and Reliability Conference 1998*, pp. 451–456, 16–19 June, Trondheim, Norway.
26. Wagner, H. Design of roof bolting patterns. Chamber of Mines workshop on roof bolting in collieries. Republic of South Africa. Johannesburg. 1985. ◆